A simple analysis of mechanism controlability and application to compliant origami design

David Dureisseix

A simple analysis of mechanism controlability and application to compliant origami design

David Dureisseix

September 22, 2016

Univ Lyon, INSA-Lyon, CNRS, LaMCoS UMR5259, F-69621, France

Abstract: Design of compliant mechanism rely on several design criteria. For instance, mechanisms using folding motions may satisfy some stiffness, strength and controlability issues. Numerical tools may help in this design phase by separating the difficulties allowing a step-by-step procedure. Herein, this separation is made by using an asymptotic expansion technique.

This is a working document of an on-going research activity. It is by no mean finalized, and content is still error-prone. It will be updated in an hopefully close future.

Keywords: compliant mechanism; mechanical design; asymptotic expansion; origami

1 Introduction

1.1 Compliant mechanisms

All structures do possess a certain degree of stiffness, defined as the force / displacement ratio, where both are measured at locations of interest, e.g. the driving or supported force is applied at a certain location, while a displacement is expected to be sufficiently large, or sufficiently small at an other location. These features or drawbacks can be estimated during structural design phase by using classical numerical tools such as finite elements.

Mechanisms are special cases where a somehow large movement is desired in the structure. Compliant mechanisms are a design solution when such a desired displacement is not too large, and when the remaining part of the structure has to sustain a load without too much other parasitic displacements. This is especially the case for precision mechanism to position or move a part with strong requirements on the accuracy. In such cases, the structure is usually weakened at some locations to mimic a mechanism for which the mobility is more or less separated from the remaining stiffness of the structure. These compliant hinges

do possess a stiffness, which is sometimes not a desirable feature (and therefore need to be carefully design and controlled), but they avoid the drawbacks of more classical linkage designs: no contact nor friction, no functional gaps...

1.2 Available models

Rigid folding is an ideal model of origami mechanism: the paper between folds is assumed to be rigid, and the folds themselves are assumed to be perfect hinges without any stiffness [2, 20].

Several designs target a mechanism with a degree one mobility, i.e. there is a single displacement mode that is compatible with the previous assumptions [4]. Usually, there are geometrical constraints to be satisfied on the fold locations, so the mechanism is hyperstatic [19]. These structures, from the historical ones made in paper [16], extended to other materials, especially for deployable structures, see [12, 13, 10, 22] for instance, or for innovative mechanisms, see [5, 6] for instance.

Command of the mechanism therefore requires theoretically only one actuator (the same number as for the mobility). It may therefore be difficult to control the movement with a single actuator due to the discrepancies with respect to the idealized model. For instance for deployable mechanism, it is much more efficient to store energy in an elastic deformation in each fold (a torsional spring) to control the unfolding of the structure.

To check the design, an evaluation of the controlability with respect to a given force actuation is proposed in the following. To keep the analysis simple, this evaluation is local to a given configuration, i.e. it analyzes the infinitesimal mechanisms close to this configuration, with respect to a given control load. For a given configuration, we model the elastic deformation with a displacement $\boldsymbol{u}$ with respect to the configuration, with the small perturbation assumption, using a finite element discretization of the given structure. The paper between folds is modeled as a thin plate, and a linear elastic behavior leads to the stiffness matrix $\boldsymbol{K}$. This matrix is singular, for which the kernel is denoted $\boldsymbol{R}$, corresponding to the modes with no energy, i.e. the rigid solid infinitesimal movements of the mobilities of the mechanism. The kernel modes stored in $\boldsymbol{R}$ are arbitrary orthonormalized as $\boldsymbol{R}^T\boldsymbol{R} = \mathbf{1}$. This model reproduced the same mechanism as the rigid folding model, and can therefore not answer to the controlability question. A perturbed model is therefore considered, for which the joints between plates are modeled as perfect hinges with a torsional elasticity distributed along the fold lines. This distribution is a weight on the repartition of resistance to movement of the mechanism: its amplitude is therefore less meaningful than its distribution. Of course, depending on the practical design of he system, the true (physical) stiffness of the joints [17] can be used.

2 Asymptotic development

The contribution of the distributed torsional spring along folds to the global stiffness matrix is $\boldsymbol{K}_1$ and the perturbation parameter is ε, so that the total stiffness matrix is $\boldsymbol{K}_\varepsilon = \boldsymbol{K} + \varepsilon \boldsymbol{K}_1$. This last one is regular, though none of $\boldsymbol{K}$ and $\boldsymbol{K}_1$ is. The amplitude of $\boldsymbol{K}_1$ is settled as similar as the amplitude of $\boldsymbol{K}$, to be precise in the following.

The load control can be separated in two components: the first one is $\boldsymbol{f}$, orthogonal to the mobilities, so that $\boldsymbol{R}^T \boldsymbol{f} = 0$, and the second one is a singular perturbation $\boldsymbol{f}_1$ that activates the mobilities. The total load is therefore $\boldsymbol{f}_\varepsilon = \boldsymbol{f} + \varepsilon \boldsymbol{f}_1$ ($\boldsymbol{f}$ and $\boldsymbol{f}_1$ having similar amplitudes). The global elastic problem is

$$\boldsymbol{K}_\varepsilon \boldsymbol{u}_\varepsilon = \boldsymbol{f}_\varepsilon \tag{1}$$

With a small parameter ε, the previous problem can be developed asymptotically [1, 18]: its solution is $\boldsymbol{u}_\varepsilon = \boldsymbol{u} + \varepsilon \boldsymbol{u}_1 + \varepsilon^2 \boldsymbol{u}_2 + \mathcal{O}(\varepsilon^3)$. This approach is close to the analyses of welded plates with a weld stiffness [9]. Different subproblems, obtained by identifying increasing powers of ε, are concerned with the different displacements as:

$$\boldsymbol{K}\boldsymbol{u} = \boldsymbol{f} \tag{2}$$
$$\boldsymbol{K}\boldsymbol{u}_1 = \boldsymbol{f}_1 - \boldsymbol{K}_1 \boldsymbol{u} \tag{3}$$
$$\boldsymbol{K}\boldsymbol{u}_2 = -\boldsymbol{K}_1 \boldsymbol{u}_1 \tag{4}$$

With a singular matrix $\boldsymbol{K}$, the solvability condition for the problem (2) is satisfied: $\boldsymbol{R}^T \boldsymbol{f} = 0$. Its solution is therefore

$$\boldsymbol{u} = \boldsymbol{K}^+ \boldsymbol{f} + \boldsymbol{R}\boldsymbol{\alpha} \tag{5}$$

$\boldsymbol{K}^+$ is a generalized inverse of $\boldsymbol{K}$ [8] and $\boldsymbol{\alpha}$ is an a priori undefined mobility mode amplitude. The problem (3) possesses a solution provided that its own solvability condition is fulfilled: $\boldsymbol{R}^T(\boldsymbol{f}_1 - \boldsymbol{K}_1 \boldsymbol{u}) = 0$. This condition leads to determine the mode amplitudes $\boldsymbol{\alpha}$ as:

$$\boldsymbol{\alpha} = \boldsymbol{k}_1^{-1} \boldsymbol{R}^T (\boldsymbol{f}_1 - \boldsymbol{K}_1 \boldsymbol{K}^+ \boldsymbol{f}) \tag{6}$$

where $\boldsymbol{k}_1 = \boldsymbol{R}^T \boldsymbol{K}_1 \boldsymbol{R}$ is the apparent stiffness of the mechanism mobilities, arising from the joint stiffness, and is regular. This gives the degree-0 solution:

$$\boldsymbol{u} = \boldsymbol{P}\boldsymbol{K}^+ \boldsymbol{f} + (\boldsymbol{R}\boldsymbol{k}_1^{-1}\boldsymbol{R}^T)\boldsymbol{f}_1 \tag{7}$$

with the projector $\boldsymbol{P} = \boldsymbol{1} - (\boldsymbol{R}\boldsymbol{k}_1^{-1}\boldsymbol{R}^T)\boldsymbol{K}_1$ on subspace span$(\boldsymbol{K}_1\boldsymbol{R})$ and in the direction span$(\boldsymbol{R})$: $\boldsymbol{P}^2 = \boldsymbol{P}$, $\boldsymbol{P}\boldsymbol{R} = 0$ and $\boldsymbol{R}^T \boldsymbol{K}_1 \boldsymbol{P} = 0$. Moreover, the solution to the problem (3) is

$$\boldsymbol{u}_1 = \boldsymbol{K}^+ (\boldsymbol{f}_1 - \boldsymbol{K}_1 \boldsymbol{u}) + \boldsymbol{R}\boldsymbol{\alpha}_1 \tag{8}$$

where the second order mode amplitudes $\boldsymbol{\alpha}_1$ are determined with the solvability condition of problem (4): $\boldsymbol{R}^T \boldsymbol{K}_1 \boldsymbol{u}_1 = 0$, as

$$\boldsymbol{\alpha}_1 = -\boldsymbol{k}_1^{-1} \boldsymbol{R}^T \boldsymbol{K}_1 \boldsymbol{K}^+ (\boldsymbol{f}_1 - \boldsymbol{K}_1 \boldsymbol{u}) \tag{9}$$

The degree-1 solution finally reads:

$$\boldsymbol{u}_1 = \boldsymbol{P}\boldsymbol{K}^+(\boldsymbol{f}_1 - \boldsymbol{K}_1\boldsymbol{u}) = (\boldsymbol{P}\boldsymbol{K}^+\boldsymbol{P}^T)(\boldsymbol{f}_1 - \boldsymbol{K}_1\boldsymbol{K}^+\boldsymbol{f}) \tag{10}$$

Both degree-0 and degree-1 solution are used to analyze the local controlability: depending on the load controls $\boldsymbol{f}$ and $\boldsymbol{f}_1$, the solutions $\boldsymbol{u}$ and $\boldsymbol{u}_1$ propagate (i.e. have an associated strain field that spans) more or less across the structure. Recalling St Venant principle [15], these solutions are localized unless the mobilities can be activated.

In each of these two displacement fields, there are two contributions: one from the regular load f and one for the activating load f_1.

3 Interpretation of the asymptotic model

Spectral analysis. To have a more clear interpretation of the contribution of the degree-0 and degree-1 solutions, a singular value decomposition [11] of the initial symmetric stiffness matrix is useful :

$$\boldsymbol{K} = \begin{bmatrix}\boldsymbol{V} & \boldsymbol{R}\end{bmatrix} \begin{bmatrix}\boldsymbol{S} & \boldsymbol{0} \\ \boldsymbol{0} & \boldsymbol{0}\end{bmatrix} \begin{bmatrix}\boldsymbol{V} & \boldsymbol{R}\end{bmatrix}^T \tag{11}$$

$\boldsymbol{S}$ is the diagonal matrix of non-zero singular values (by decreasing order), $\boldsymbol{V}$ is a rotated orthonormal basis of the regular subspace of the stiffness matrix, orthogonal to the kernel $\boldsymbol{R}$. Then, $\boldsymbol{K} = \boldsymbol{V}\boldsymbol{S}\boldsymbol{V}^T$ and $\boldsymbol{K}^+ = (\boldsymbol{V}\boldsymbol{S}\boldsymbol{V}^T + \boldsymbol{R}\gamma\boldsymbol{R}^T)^{-1} = \boldsymbol{V}\boldsymbol{S}^{-1}\boldsymbol{V}^T + \boldsymbol{R}\gamma^{-1}\boldsymbol{R}^T$ where $\gamma > 0$ is used as a regularization.

If one represents the regular load as $\boldsymbol{f} = \boldsymbol{V}\boldsymbol{S}\boldsymbol{g}$ (i.e. in span($\boldsymbol{V}$)) and the singular load as $\boldsymbol{f}_1 = \boldsymbol{R}\boldsymbol{k}_1\boldsymbol{g}_1$ (i.e. in span($\boldsymbol{R}$)), one gets indeed $\boldsymbol{R}^T\boldsymbol{f} = 0$ and also $\boldsymbol{V}^T\boldsymbol{f}_1 = 0$; this is a unique decomposition of any arbitrary load. One then obtains: $\boldsymbol{P}\boldsymbol{K}^+\boldsymbol{f} = \boldsymbol{P}\boldsymbol{V}\boldsymbol{g}$, and $\boldsymbol{R}\boldsymbol{k}_1^{-1}\boldsymbol{R}^T\boldsymbol{f}_1 = \boldsymbol{R}\boldsymbol{g}_1$. Finally, the degree-0 solution is

$$\boldsymbol{u} = \begin{bmatrix}\boldsymbol{V} & \boldsymbol{R}\end{bmatrix} \begin{bmatrix}\boldsymbol{g} \\ \boldsymbol{g}_1^\star\end{bmatrix} \tag{12}$$

where $\boldsymbol{g}_1^\star = \boldsymbol{g}_1 - \boldsymbol{k}_1^{-1}(\boldsymbol{R}^T\boldsymbol{K}_1\boldsymbol{V})\boldsymbol{g}$ is a condensed vector, and the degree-1 solution is

$$\begin{aligned}\boldsymbol{u}_1 &= \boldsymbol{P}\boldsymbol{V}\boldsymbol{S}^{-1}\left\{(\boldsymbol{V}^T\boldsymbol{K}_1\boldsymbol{R})\boldsymbol{g}_1 + \boldsymbol{K}_1^\star\boldsymbol{g}\right\} = \\ &= \begin{bmatrix}\boldsymbol{V} & \boldsymbol{R}\end{bmatrix} \begin{bmatrix}\boldsymbol{1} \\ -\boldsymbol{k}_1^{-1}(\boldsymbol{R}^T\boldsymbol{K}_1\boldsymbol{V})\end{bmatrix} \boldsymbol{S}^{-1}\left\{(\boldsymbol{V}^T\boldsymbol{K}_1\boldsymbol{R})\boldsymbol{g}_1 + \boldsymbol{K}_1^\star\boldsymbol{g}\right\}\end{aligned} \tag{13}$$

where $\boldsymbol{K}_1^\star = (\boldsymbol{V}^T\boldsymbol{K}_1\boldsymbol{V}) - (\boldsymbol{V}^T\boldsymbol{K}_1\boldsymbol{R})\boldsymbol{k}_1^{-1}(\boldsymbol{R}^T\boldsymbol{K}_1\boldsymbol{V})$ is a condensed stiffness matrix.

A load with a priori no mobility activation. The first particular case that can be discussed concerns a load with only a regular component, i.e. $\boldsymbol{g}_1 = 0$.

The solutions read:

$$\boldsymbol{u} = \begin{bmatrix} \boldsymbol{V} & \boldsymbol{R} \end{bmatrix} \begin{bmatrix} \mathbf{1} \\ -\boldsymbol{k}_1^{-1}(\boldsymbol{R}^T \boldsymbol{K}_1 \boldsymbol{V}) \end{bmatrix} \boldsymbol{g} \tag{14}$$

$$\boldsymbol{u}_1 = \boldsymbol{P}\boldsymbol{V}\boldsymbol{S}^{-1}\boldsymbol{K}_1^\star \boldsymbol{g} = \begin{bmatrix} \boldsymbol{V} & \boldsymbol{R} \end{bmatrix} \begin{bmatrix} \mathbf{1} \\ -\boldsymbol{k}_1^{-1}(\boldsymbol{R}^T \boldsymbol{K}_1 \boldsymbol{V}) \end{bmatrix} \boldsymbol{S}^{-1}\boldsymbol{K}_1^\star \boldsymbol{g} \tag{15}$$

Therefore, the degree-0 solution $\boldsymbol{u}$ has indeed a plate deformation component with the term $\boldsymbol{V}\boldsymbol{g}$, but due to the coupling stiffness $\boldsymbol{R}^T\boldsymbol{K}_1\boldsymbol{V}$, it also activates a mechanism mobility with the second term. The degree-1 correction has the same structure, with $\boldsymbol{g}$ replaced with $\boldsymbol{S}^{-1}\boldsymbol{K}_1^\star\boldsymbol{g}$, which entirely depends on the same coupling stiffness in $\boldsymbol{K}_1^\star$.

A load with a priori only the mobility activation. The complementary example is when $\boldsymbol{g} = 0$, so that $\boldsymbol{u} = \boldsymbol{R}\boldsymbol{g}_1$ (as for a rigid plate case) and $\boldsymbol{u}_1 = \boldsymbol{P}(\boldsymbol{V}\boldsymbol{S}^{-1}\boldsymbol{V}^T)\boldsymbol{K}_1\boldsymbol{u}$.

Influence of coupling stiffness terms. The coupling stiffness $\boldsymbol{V}^T\boldsymbol{K}_1\boldsymbol{R}$ is leading the different terms. With the stiffness repartition along the fold lines, the stiffness $\boldsymbol{K}_1$ is not restricted to the sole mechanism mobility modes, e.g. the stiffness $\boldsymbol{k}_1 = \boldsymbol{R}^T\boldsymbol{K}_1\boldsymbol{R}$, and the coupling term is not zero. If this was the case, the previous expressions simplify into:

$$\boldsymbol{u} = \begin{bmatrix} \boldsymbol{V} & \boldsymbol{R} \end{bmatrix} \begin{bmatrix} \boldsymbol{g} \\ \boldsymbol{g}_1 \end{bmatrix} \tag{16}$$

$$\boldsymbol{u}_1 = \boldsymbol{V}\boldsymbol{S}^{-1}(\boldsymbol{V}^T\boldsymbol{K}_1\boldsymbol{V})\boldsymbol{g} \tag{17}$$

Moreover, a zero coupling term will also lead to $\boldsymbol{V}^T\boldsymbol{K}_1\boldsymbol{V} = 0$ (no influence on the regular stiffness of the plates) and the degree-1 displacement is null: $\boldsymbol{u}_1 = 0$. The total displacement therefore reduces to $\boldsymbol{u}$ with two separated contributions: the plate deformation mode $\boldsymbol{V}\boldsymbol{g}$ and the mobility movement $\boldsymbol{R}\boldsymbol{g}_1$. It is therefore a simple superposition of the rigid folding mechanism model, and the plate deformation model, that does not serve the purpose of checking the controlability.

Rigid cases. The rigid plate model corresponds to selecting $\boldsymbol{S}^{-1} = 0$. In this case, the solutions reduce to: $\boldsymbol{u} = \boldsymbol{R}\boldsymbol{g}_1^\star$ and $\boldsymbol{u}_1 = 0$. For the rigid origami model, one adds $\boldsymbol{K}_1 = 0$, so that $\boldsymbol{g}_1^\star = \boldsymbol{g}_1$. This is a pure mechanism mobility mode, and does not allow as well a controlability estimation.

4 Controlability estimation

To get useful information on the controlled structure, we therefore rely on the perturbed compliant model, i.e. with a stiffness repartition along the fold lines.

If no additional information is provided, a uniform repartition en selected as a perturbation. The analysis is specific to a given load control $\boldsymbol{f}_t$ in a given configuration. It is separated in two contributions, $\boldsymbol{f}_1 = \boldsymbol{R}\boldsymbol{R}^T\boldsymbol{f}_t$ and $\boldsymbol{f} = \boldsymbol{f}_t - \boldsymbol{f}_1$. The costly part requires two global solves to get the system answer $(\boldsymbol{u}, \boldsymbol{u}_1)$ from (7) and (10).

The controlability question can be addressed by using an analogy with strain field propagation in continuum mechanics. Indeed, the so-called St Venant principle provides a general result on propagation of edge effects: if an elastic solid is loaded with a residual (i.e. with a null resultant and a null resulting torque), the deformation is localized in the vicinity of the load.

There are noticeable counter-examples or special cases, for instance, some structures with incompressible or quasi-incompressible material, such as the slab in Figure 1, where the load on a face propagates the strain up to the opposite face; some thin-walled structures [14, 21] Figure 2. We also expect that with a controllable compliant mechanism, a command at some point may propagate along the mechanism with its mobility to reach with sufficient amplitude the part that is intended to be controlled.

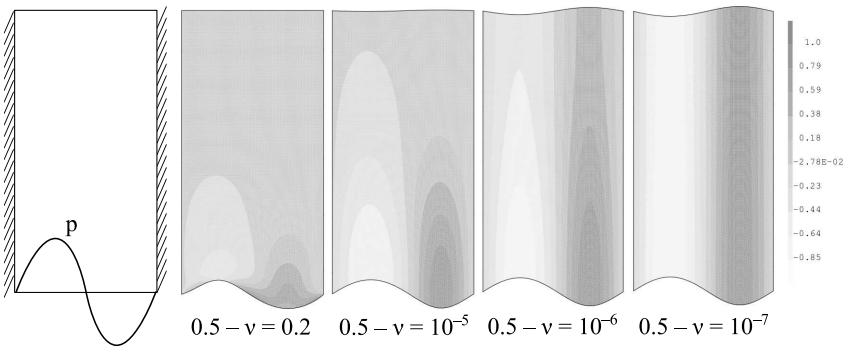

Figure 1: Elastic slab (laterally clamped) submitted to a bottom sine pressure and with a free top side, for cases closer and closer to incompressibility (plane deformation, vertical normalized deformation is depicted on the normalized deformed configuration).

4.1 Implementation issues

For an implementation point of view, the kernel of the stiffness matrix $\boldsymbol{K}$ as well as the factorization of its regularized version benefit of the approach used for floating substructures [7, 3].

Dealing with plate finite elements, for instance DKT, care must be taken with the hybrid nature of the degrees of freedom (displacements and rotations), so a diagonal scaling may be applied prior to the factorization. This is especially useful when using a fictitious small stiffness for the drilling local rotations, normal to the plate element, to avoid non-physical modes with zero stiffness.

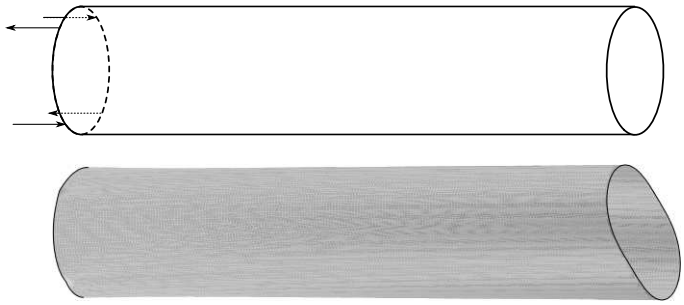

Figure 2: Elastic thin tube loaded with traction and compression forces of null resultant and resulting torque.

For the additional perturbation stiffness $\boldsymbol{K}_1$, this can be issued from a stiffener model of the interface between plates. Considering again the solution technology used for domain decomposition, one car consider each plate panel as an independent subdomain, A boolean mapping matrix on the interface reads: $\boldsymbol{B}_u$ for transferring the dof of the plates to the displacement jump on the interface, and $\boldsymbol{B}_r$ for transferring the dof of the plates to the rotation jump on the interface. Assembling the plates in a mechanism fashion leads to (i) nullify the displacement jump, i.e. prescribing $\boldsymbol{B}_u\boldsymbol{u} = 0$ (for instance by dof substitution method), and (ii) to define rotation jumps on the nodes of the stiffener elements (beam elements for instance, as in []), as $\Delta\boldsymbol{\omega} = \boldsymbol{B}_r\boldsymbol{u}$. The stiffness $\boldsymbol{K}_1$ is the assembly of a beam stiffness with only a distributed torsional stiffness behavior, as $\boldsymbol{K}_1 = \boldsymbol{B}_r^T\boldsymbol{\kappa}\boldsymbol{B}_r$.

Normalization. For conditioning issues, we choose to modify the stiffness matrices using a diagonal scaling. Moreover, the amplitude of the two stiffness matrices are to be chosen similar.

To do so, we first consider the stiffness matrix $\boldsymbol{K}$, which is singular, but as a full assembling of elementary stiffness matrices, possess positive non-null diagonal terms. The scaling is therefore a diagonal matrix $\boldsymbol{W}$ storing the inverse of the square root of the diagonal terms of the initial matrix, i.e. $\boldsymbol{W} = (\boldsymbol{K}^D)^{-1/2}$. The renormalized matrix is therefore $\widetilde{\boldsymbol{K}} = \boldsymbol{W}\boldsymbol{K}\boldsymbol{W}$. It is still singular, with a kernel $\widetilde{\boldsymbol{R}}$ (that can be chosen such that $\widetilde{\boldsymbol{R}}^T\widetilde{\boldsymbol{R}} = \boldsymbol{1}$). A suited generalized inverse could be $\widetilde{\boldsymbol{K}}^+ = (\widetilde{\boldsymbol{K}} + \widetilde{\boldsymbol{R}}\widetilde{\boldsymbol{R}}^T)^{-1}$.

The stiffness matrix $\boldsymbol{K}_1$ is also singular but is only a partial assembling of elementary matrices, and therefore exhibits null diagonal terms. The amplitude of this matrix is chosen such that the mean value of the non-null diagonal terms corresponding to rotations in $\boldsymbol{K}_1$ is equal to the same mean for $\boldsymbol{K}$. Then, the scaling for $\boldsymbol{K}_1$ is also selected as $\boldsymbol{W}$ and $\widetilde{\boldsymbol{K}}_1 = \boldsymbol{W}\boldsymbol{K}_1\boldsymbol{W}$.

Due to the simultaneous scaling of the two stiffness matrices, the previous

approach is trivially applied to the renormalized system, that is:

$$\widetilde{\boldsymbol{K}}\boldsymbol{v} = \boldsymbol{g} \quad \text{with} \quad \boldsymbol{g} = \boldsymbol{W}\boldsymbol{f} \quad \text{and} \quad \boldsymbol{u} = \boldsymbol{W}\boldsymbol{v} \tag{18}$$

$$\widetilde{\boldsymbol{K}}\boldsymbol{v}_1 = \boldsymbol{g}_1 - \widetilde{\boldsymbol{K}}_1\boldsymbol{v} \quad \text{with} \quad \boldsymbol{g}_1 = \boldsymbol{W}\boldsymbol{f}_1 \tag{19}$$

$$\widetilde{\boldsymbol{K}}\boldsymbol{v}_2 = -\widetilde{\boldsymbol{K}}_1\boldsymbol{v}_1 \tag{20}$$

so that: $\boldsymbol{v} = \boldsymbol{v}_{\rm reg} + \boldsymbol{v}_{\rm mec}$ and $\boldsymbol{v}_1 = \boldsymbol{v}_{1,\rm reg} + \boldsymbol{v}_{1,\rm mec}$ with

$$\boldsymbol{v}_{\rm reg} = \widetilde{\boldsymbol{P}}\widetilde{\boldsymbol{K}}^{+}\boldsymbol{g} \tag{21}$$

$$\boldsymbol{v}_{\rm mec} = \widetilde{\boldsymbol{R}}\widetilde{\boldsymbol{k}}_1^{-1}\widetilde{\boldsymbol{R}}^{T}\boldsymbol{g}_1 \tag{22}$$

$$\boldsymbol{v}_{1,\rm reg} = -\widetilde{\boldsymbol{P}}\widetilde{\boldsymbol{K}}^{+}\widetilde{\boldsymbol{K}}_1\boldsymbol{v}_{\rm reg} = -\widetilde{\boldsymbol{P}}\widetilde{\boldsymbol{K}}^{+}\widetilde{\boldsymbol{P}}^{T}\widetilde{\boldsymbol{K}}_1\widetilde{\boldsymbol{K}}^{+}\boldsymbol{g} \tag{23}$$

$$\boldsymbol{v}_{1,\rm reg} = \widetilde{\boldsymbol{P}}\widetilde{\boldsymbol{K}}^{+}\widetilde{\boldsymbol{P}}^{T}\boldsymbol{g}_1 \tag{24}$$

and $\widetilde{\boldsymbol{P}} = \boldsymbol{1} - (\widetilde{\boldsymbol{R}}\widetilde{\boldsymbol{k}}_1^{-1}\widetilde{\boldsymbol{R}}^{T})\widetilde{\boldsymbol{K}}_1$ with $\widetilde{\boldsymbol{k}}_1 = \widetilde{\boldsymbol{R}}^{T}\widetilde{\boldsymbol{K}}_1\widetilde{\boldsymbol{R}}$.

4.2 Design indicators

Once the solution $\boldsymbol{u}_{\rm reg}$ is obtained, it can be used to check a first feature: when no driving force is applied, $\boldsymbol{f}_1 = 0$ (so that $\boldsymbol{u}_1 = 0$), does load $\boldsymbol{f}$ to be sustained induces parasitic displacement? Indeed, $\boldsymbol{u}_{\rm reg}$ is expected to satisfy the Saint Venant principle and should be more or less localized in the neighborhood of the load. Its long range propagation would have therefore to be limited in the design of the compliant structure.

On the other hand, with $\boldsymbol{u}_{\rm mec}$, the target is to have a sufficient propagation of the mobility movement to mimic a mechanism that is under target. This time, the displacement propagation should be sufficiently developed.

Once the configuration of the compliant structure (position of panels, hinges...) has been selected based on the previous indicators, the parameter ε can now be chosen. Indeed, the asymptotic analysis if performed ideally when $\varepsilon \to 0$, but in each design, ε has a finite value. For the designer, a target value can be obtained by selecting the design of the hinges (thickness, material...) or of the panels. ε is typically the relative stiffness of the most compliant parts and the most rigid parts of the structure. Design intervals for its value can therefore be selected when comparing the indicators $\boldsymbol{u}_{\rm reg}$ and $\boldsymbol{u}_{\rm mec}$ to the next order indicators $\boldsymbol{u}_{1,\rm reg}$ and $\boldsymbol{u}_{1,\rm mec}$ discussing the structural performance compromises, since $\boldsymbol{u}_{t,\rm reg} \approx \boldsymbol{u}_{\rm reg} + \varepsilon\boldsymbol{u}_{1,\rm reg}$ and $\boldsymbol{u}_{t,\rm mec} \approx \boldsymbol{u}_{\rm mec} + \varepsilon\boldsymbol{u}_{1,\rm mec}$.

Finally, the absolute stiffness can be found as the threshold of the indicators as the answer of the structure submitted to the given amplitude of the load.

References

[1] A. Bensoussan, J.-L. Lions, and G. Papanicolaou. *Asymptotic Analysis for Periodic Structures*. North Holland, Amsterdam, 1978.

[2] E. D. Demaine and J. O'Rourke. *Geometric Folding Algorithms: Linkages, Origami, Polyhedra*. Cambridge University Press, New York, NY, USA, 2008.

[3] I. S. Duff. MA57—a code for the solution of sparse symmetric definite and indefinite systems. *ACM Trans. Math. Softw.*, 30(2):118–144, June 2004. URL: http://doi.acm.org/10.1145/992200.992202, doi:10.1145/992200.992202.

[4] D. Dureisseix. An overview of mechanisms and patterns with origami. *International Journal of Space Structures*, 27(1):1–14, 2012. URL: http://multi-science.atypon.com/doi/abs/10.1260/0266-3511.27.1.1, doi:10.1260/0266-3511.27.1.1.

[5] R. A. Evans, R. J. Lang, S. P. Magleby, and L. L. Howell. Rigidly foldable origami twists. In *Origami 6*, volume 1, pages 119–130. American Mathematical Society, 2015.

[6] T. A. Evans, R. J. Lang, S. P. Magleby, and L. L. Howell. Rigidly foldable origami gadgets and tessellations. *R. Soc. open sci.*, 2:150067, 2015. doi:10.1098/rsos.150067.

[7] C. Farhat and M. Géradin. On the general solution by a direct method of a large-scale singular system of linear equations: Application to the analysis of floating structures. *International Journal for Numerical Methods in Engineering*, 41(4):675–696, 1998. doi:10.1002/(SICI)1097-0207(19980228)41:4<675::AID-NME305>3.0.CO;2-8.

[8] C. Farhat and D. Rixen. *Encyclopedia of Vibration*, chapter Linear Algebra, pages 710–720. Academic Press, 2002.

[9] G. Geymonat and F. Krasucki. Analyse asymptotique du comportement en flexion de deux plaques collées. *Comptes Rendus de l'Académie des Sciences de Paris*, 325(325):307–314, 1997. Série IIb. In French.

[10] F. Gioia, D. Dureisseix, R. Motro, and B. Maurin. Design and analysis of a foldable/unfoldable corrugated architectural curved envelop. *Journal of Mechanical Design*, 134(3):031003(1–12), 2012. URL: http://link.aip.org/link/?JMD/134/031003/1http://mechanicaldesign.asmedigitalcollection.asme.org/article.aspx?articleid=1450770, doi:10.1115/1.4005601.

[11] G. H. Golub and C. F. Van Loan. *Matrix Computations*. The Johns Hopkins University Press, 4th edition, 2012.

[12] S. D. Guest and S. A. De Focatiis. Deployable membranes designed from folding tree leaves. *Philosophical Transactions of the Royal Society. Mathematical, physical and engineering sciences*, 360(1791):227–238, 2002.

[13] K. Kuribayashi, K. Tsuchiya, Z. You, D. Tomus, M. Umemoto, T. Ito, and M. Sasaki. Self-deployable origami stent grafts as a biomedical application of Ni-rich TiNi shape memory alloy foil. *Materials Science and Engineering: A*, 419(1-2):131–137, 2006. URL: http://www.sciencedirect.com/science/article/B6TXD-4J55650-4/2/7659f576ead94489c2b4daad3d3689c2, doi:10.1016/j.msea.2005.12.016.

[14] P. Ladevèze, P. Sanchez, and J. G. Simmonds. Beamlike (Saint-Venant) solutions for fully anisotropic elastic tubes of arbitrary closed cross section. *International Journal of Solids and Structures*, 41(7):1925–1944, 2004. URL: http://www.sciencedirect.com/science/article/B6VJS-4B8K93J-6/2/38355ab5648ca2da239abd41be1fc0cd, doi:DOI:10.1016/j.ijsolstr.2003.11.006.

[15] J. Lemaitre. Résistance des matériaux. http://www.universalis.fr/encyclopedie/resistance-des-materiaux/. Accessed: 2016-09-22. Encyclopædia Universalis [online].

[16] K. Miura. *Map fold a la Miura style, its physical characteristics and application to the space science*, pages 77–90. Research of Pattern Formation. KTK Scientific Publishers, 1993.

[17] C. Pradier, J. Cavoret, D. Dureisseix, C. Jean-Mistral, and F. Ville. An experimental study and model determination of the mechanical stiffness of paper folds. *Journal of Mechanical Design*, 138(4):041401, 2016. doi:10.1115/1.4032629.

[18] E. Sanchez-Palencia. *Non homogeneous media and vibration theory*, volume 127 of *Lecture Notes in Physics*. Springer Verlag, 1980.

[19] J. E. Shigley and J. J. Uicker. *Theory of Machines and Mechanisms*. McGraw-Hill, New York, 2nd edition, 1995.

[20] T. Tachi. Simulation of rigid origami. In *Fourth International Conference on Origami in Science, Mathematics, and Education — 4OSME*, pages 175–187, 2009.

[21] V. Z. Vlasov. *Thin-Walled Elastic Beams*. Moscow, 2nd edition, 1959. English translation published for U. S. Science Foundation by Israel Program for Scientific Translations, Jerusalem, 1961; original title: Tonkostennye uprugie sterzhni.

[22] S. A. Zirbel, R. J. Lang, M. W. Thomson, D. A. Sigel, P. E. Walkemeyer, B. P. Trease, S. P. Magleby, and L. L. Howell. Accommodating thickness in origami-based deployable arrays. *Journal of Mechanical Design*, 135:111005(1–11), 2013. doi:10.1115/1.4025372.